Pure Appl. Chem., Vol. 74, No. 11, pp. 2119–2129, 2002.

Engineering and chemistry of the glass-melting process*

Lubomír Němec‡

Laboratory of Inorganic Materials, Joint Workplace of the Institute of Inorganic Chemistry of ASCR and the Institute of Chemical Technology, Technická 5, 166 28 Prague 6, Czech Republic

Abstract: Improved glass-melting technology, intelligent process control, glass quality control, and establishing novel melting conditions, are realized by different kinds of physicochemical models. The model application is preceded by the analysis of homogenization processes, i.e., heating, dissolution, or vitrification and refining. The energy consumption of the process, the pull rate and size of the melting space, and glass quality are the main technological factors taken into account. In the following step, the optimum conditions are applied to simplified and complex models or processes. The mentioned models are mostly represented by systems containing melt and numerous inhomogeneities (solid particles, bubbles).

INTRODUCTION

The industrial glass-melting process involves a set of chemical, physicochemical, and physical processes that can be best described and controlled by applying a chemico-engineering approach; this approach is manifested by different kinds of models, including mathematical, experimental, and combined models [1]. The main aims of modeling are improved glass-melting technology, intelligent process control and glass quality control, as well as setting up new glass-melting conditions and facilities. The new trends in this field involve the analysis of process leading to the estimation of the best melting conditions, the formation of simplified models of the melting and vitrification process, and the formation of complex models describing glass quality. This paper presents a short review of these trends.

ANALYSIS OF THE GLASS-MELTING PROCESS

The classical glass-melting process includes two main processes—heating and homogenization. Homogenization is the complex process involving dissolution of solid and liquid inhomogeneities and removing bubbles. In most cases, the processes are mostly ordered as a sequence: heating → dissolution → bubble removing (refining).

It seems useful to describe the main processes by simple equations for the purpose of process analysis. Consequently, the heating process may be described by the conductive and radiation heat transfer into a solid material (glass batch):

$$\dot{Q} = \sum_{i=1}^{n} A_i \frac{\lambda_i}{\delta_i}\left(T^{m_i} - T^{b_i}\right) + C\Delta T^4 \qquad (1)$$

*Lecture presented at the 5th Conference on Solid State Chemistry (SSC 2002), Bratislava, Slovakia, 7–12 July 2002. Other presentations are published in this issue, pp. 2083–2168.

‡E-mail: nemec@iic.cas.cz

where $\dot{Q}$ is the heat flow into the batch, A_i is the ith part of the batch surface, λ_i is the heat conductivity of heating medium, δ_i is the thickness of the heating layer, T^{m_i} is the bulk temperature of the heating medium, T^{b_i} is the temperature of the batch surface, and C is the heat-transfer coefficient of radiation.

The particle behavior involving the dissolution of solid particles and the behavior of bubbles may be in a simplified form described by the Noyes–Nernst equation:

$$\frac{da}{d\tau} = \frac{D}{\rho_P \delta}(C_b - C_{eq}) \tag{2}$$

where τ is time, a is the particle size (mostly radius), D is the diffusivity of transferred component, ρ_P is the particle density, δ is the diffusion layer thickness, C_b is the bulk concentration, and C_{eq} is the surface equilibrium concentration of transferred component. For the dissolution process, $C_b > C_{eq}$, for bubbles are the main mechanism of their growth, i.e., $C_b > C_{eq}$.

The refining or vitrification processes are realized by rising growing bubbles to the level or by crystals settling, and Stokes' relation may be mostly applied:

$$v_{bub} = \frac{2g\Delta\rho}{9\eta} a^2(\tau) \tag{3}$$

where v_{bub} is the bubble-rising velocity, $\Delta\rho$ is the density difference between particle and melt, and η is the dynamic viscosity of glass melt.

The fundamental technological parameters involve then the specific energy consumption of the process, the pull rate of the melting space, volume space (facility size), and quality (homogeneity) of glass. For the entire melting process, the specific energy consumption may be in a simplified form written as [2]:

$$H_M^0 = H_M^G + C^G\left(T^{max} - T^e\right) + \frac{\dot{H}_T^L\left(T^{in} - T^{ex}\right)}{P} \tag{4}$$

where H_M^G includes reaction, phase transformation, and evaporation heats, as well as enthalpy to heat the batch and glass to the furnace exit temperature, T^e, C^G is the glass heat capacity, T^{max} is the maximum melting temperature, $\dot{H}_T^L$ is the heat flux through boundaries related to the unit temperature gradient, P is the pull rate of the space, and T^{in} and T^{ex} are the average inner and outer temperatures of space walls, respectively.

While the pull rate of heating is given by the heat absorbed in batch:

$$P^{Heat} = \frac{\dot{Q}}{H_M^G + C^G\left(T - T^e\right)} \tag{5}$$

where T is the temperature attained in the heating region, the pull rates of dissolution and refining are bound with process chemistry and kinetics:

$$P^{Diss,Ref} = \frac{\rho V(1-m)}{\bar{\tau}} \tag{6}$$

where V is the volume, m is the fraction of the dead volume (quiescent glass, rotating glass), and $\bar{\tau}$ is the average residence time of glass to accomplish dissolution or refining.

For the refining process, the value of m is close to zero and the value of $\bar{\tau} \geq \tau_{crit}^{Ref}$, where τ_{crit}^{Ref} is the critical time of refining. The value of $\bar{\tau}$ for the dissolution process may be given by:

$$\bar{\tau} \geq K_Q \bar{\tau}_{Diss} \tag{7}$$

where $\bar{\tau}_{\mathrm{Diss}}$ is the average dissolution time of particles and $K_Q \geq 1$ is the constant expressing under given conditions the differences in dissolution histories of different particles (different dissolution quality of single pathways).

The presented simplified equations allow us to determine the potentially beneficial conditions of the process. Equation 4 shows results that the specific energy consumption decreases with the growing pull rate, and eq. 6 predicts the possible miniaturization of the melting space; the pull rate could be increased by enhanced melting kinetics (decrease in $\bar{\tau}$).

The analysis of the heating process leads to the conclusion that the main intensifying factor is the dispersion of the batch in the heating medium, the intensive glass convection under the batch blanket joint with submerged combustion (physical factors), and reducing or removing the bubble layer under the batch blanket (physical and chemical factors). More sophisticated models of glass batch decomposition and melting are needed. The contemporary requirements on the dissolution process are aimed at melt stirring and flow control, the first factor enhances the dissolution process, the second one decreases the fraction of the dead room if the proper combination of piston flow and perfect mixing was applied (quasi-piston flow) [3]. The utilization of the mentioned factors is the direct challenge to modeling dissolution processes under real conditions. The modern trends in the refining process lead either to very high refining temperatures (but also high energy consumption) or to the refining process accomplished at medium temperatures and low levels of both refining agents (favorable ecological effect) and pressure. The appropriate models and modeling are here needed, too. The still-open question of both dissolution and refining process is the application of microstirring to enhance processes, i.e., microwave boosting [4] or chemical stirring by nucleated bubbles. The development of the appropriate physicochemical models seems, therefore, a necessary subsequent step of progress in the field.

SIMPLIFIED MODELS

The analysis of the glass-melting process provides special conditions for single processes, namely heating, dissolution, refining, and vitrification involving crystal settling. Using this knowledge, simplified models can be derived to predict the process development under a priori defined conditions. Subsequently, the best results may be applied to more complicated real conditions by using complex models. Such simplified models were developed especially for processes taking part in the melt.

Dissolution

The analysis of the dissolution process provides special dissolution conditions: The mainstream of glass simulates the piston flow, but the melt is intensively mixed in planes perpendicular to the mainstream (quasi-piston flow). The local concentration of undissolved particles in the space with quasi-piston flow is given by [5]:

$$C' = C_{\mathrm{in}} \int_{a_0 \min}^{a_0 \max} f(a_0) \frac{a^3(a_0, \tau)}{a_0^3} da_0; \frac{da}{d\tau} = k_H \left(C - \frac{C'}{\rho_{\mathrm{p}}} \right) \tag{8a,b}$$

where C_{in} is input mass concentration of particles, a_0 and a are initial and instant particle sizes, C_0 is the equilibrium volume fraction of dissolving particles in the melt, ρ_p is particle density, and k_H is the mass transfer coefficient dependent on the intensity of glass convection in planes perpendicular to the main stream. $f(a_0)$, the probability density function of particle size distribution, expresses the polydispersity of particles, eq. 8b is the Hixon–Crowel equation. If $C' \rightarrow 0$, $\tau = \tau_{\mathrm{Diss}}$ (see eq. 7). Thus, the energy consumption and pull rate of the dissolution channel of constant size and with quasi-piston flow can be calculated from eqs. 4 and 6. Figure 1 presents the results for the model dissolution space

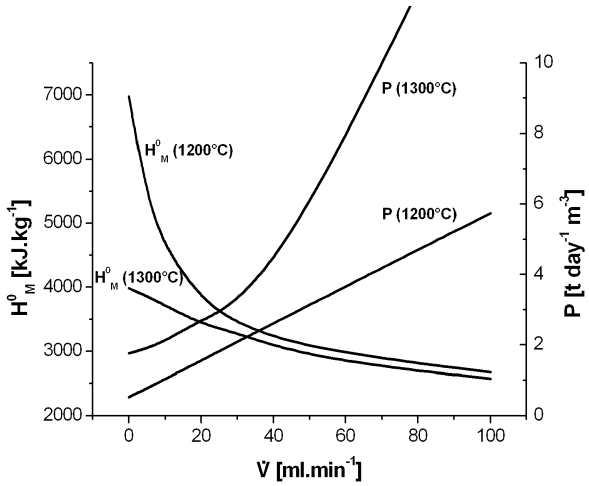

Fig. 1 Effect of glass stirring on the specific energy consumption and specific pull rate when heating and melting soda-lime-silica glass in a model melting space. The stirring intensity is represented by the amount $\dot{v}$ of stirring gas bubbled into the laboratory crucible, temperatures 1200 and 1300 °C, respectively, $(1 - m)/K_Q = 0.2$ (see eqs. 6 and 7).

($V = 1$ m^3) in the form of dependence between H_M^0, respectively P_{Diss}, and the intensity of glass convection for temperatures 1200 and 1300 °C.

The main goal of the high-level waste (HLW) vitrification process is prevention of spinel crystal settling on the bottom of vitrification space. The results of the 3-D numerical mathematical model have shown that the majority of the vitrification space behaves as a perfect mixer [6], and the steady concentration of dissolving crystals may be obtained from the mass balance of crystals. The rate of the layer growth is then given by [7]:

$$\frac{dh_{\text{cr}}}{d\tau} = \frac{0.205 g \Delta\rho C_{\text{in}} \dot{V}}{\eta V C_{\text{layer}}} \int_0^{\infty} \exp\left(-\frac{\dot{V}}{V}\tau\right)\left[a_0 + k_H\left(C_0 - \frac{C}{\rho_{\text{p}}}\right)\tau\right]^5 d\tau \tag{9}$$

where h_{cr} is the layer thickness, V is the volume pull rate of the space, and C is the steady concentration of crystals in the melter.

The results have shown that arranging piston flow under the batch blanket prior to perfect mixing may provide conditions that reduce or prevent the crystal layer formation. Figure 2 shows the decrease of the crystal layer thickness after one year of melter operation when prolonging the initial piston flow period. In the limiting case of $\tau_p = \tau_{\text{Diss}}$ (τ_p is duration of the piston flow period), all crystals dissolve before entering the perfectly mixed space, i.e., the crystal layer is not created.

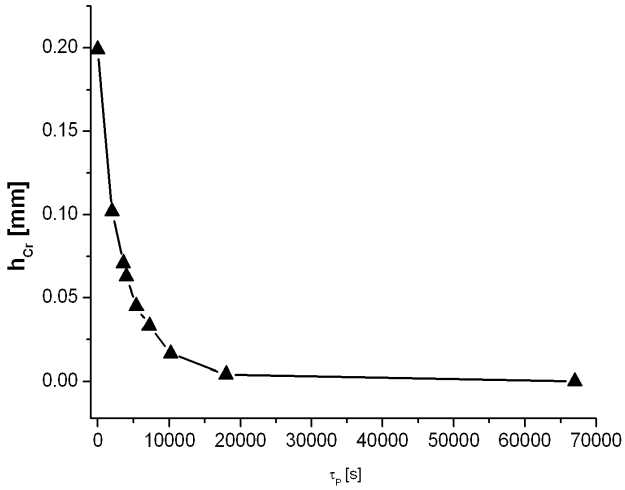

Fig. 2 Dependence of thickness of the spinel crystal layer on the length of the piston flow period under batch blanket.

Refining

The effective realization of the bubble-removing process by rising to the level applies for piston flow and fast-growing bubbles. As already mentioned, both high temperatures and low pressures fulfill these conditions [8]. The local concentration of growing bubbles in a space with piston flow can be calculated from trajectories of single bubbles of defined initial size. For bubbles of initial size distribution $f(a_0)$ and initial concentration N (number of bubbles per volume or mass unit of glass), their concentration in the given point x, z is described by:

$$C(x,z) = \tfrac{4}{3}\pi\rho_s N \int_{a_{0\min}}^{a_{0\max}} f(a_0)(a_0 + \dot{a}\tau)^3 da_0; \tau = \frac{x}{v_{\mathrm{gl}}} \qquad (10a,b)$$

where v_{gl} is the constant value of glass velocity, $\dot{a}$ is the constant value of bubble growth rate, $a'_{0\min}$ and $a'_{0\max}$ are the minimum and maximum radii of particles crossing the given point [x, z] in time τ.

Figure 3 shows the specific energy consumption and specific pull rate when removing bubbles from a model refining space (V = 1 m^3) having constant height and working under different pressures. The clearly beneficial effect of reduced pressure on both energy consumption and pull rate is obvious.

As the presented examples show, the applications of simplified models working under isothermal conditions and simple flow conditions—piston flow or perfect mixer—can reliably reveal the significance of beneficial factors, derived from the process analysis. The following step, however, has to aim at factor application in more complicated real conditions.

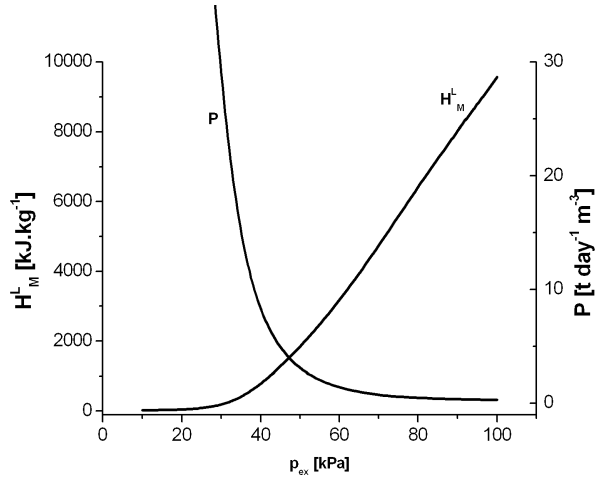

Fig. 3 Effect of pressure on the specific energy consumption and specific pull rate when refining soda-lime-silica glass in a model melting space with constant height. Temperature 1200 °C.

COMPLEX MODELS DESCRIBING GLASS QUALITY

The complex models are created with the aim to face the main problems of industrial glass melting; the quality models are always a substantial item of the complex model approach [9,10]. Bubbles and stones or crystals, coming from the batch-melting and secondary sources of inhomogeneities, undergo a series of processes, some of them not being adequately described by equations: initiation mechanisms, process linking (e.g., bubble nucleation on liquid or solid inhomogeneities), mutual impact of inhomogeneities (coalescence, aggregation, flotation), or mutual influence of inhomogeneity files and melt (heat and mass transfer). The quality models involve, on the contrary, behavior of the melt (temperature and velocity distribution), kinetic behavior of single and numerous inhomogeneities, and the influence of inhomogeneities on the melt flow due to buoyancy force. Scheme 1 brings the schema of the complex model of glass quality working under real conditions. The contemporary models of melting in the batch blanket do not follow the histories of single particles, that is why the presented model applies the experimental modeling of batch-melting and secondary sources in laboratory conditions (boxes B1 and B2) using the time-temperature regimes in the batch obtained from the modeling of pure melt and batch behavior (boxes C1 and A). Thus, the initial numbers, sizes, and compositions of solid and gas inhomogeneities are acquired. The particle distribution in the melting space is calculated using the diffusion–convective mass transfer equation (box C2), supplied by melt-temperature and velocity data from C1 and kinetic data of single inhomogeneity behavior from boxes D1–D3, respectively E (crystal layer growth during the vitrification process). Simultaneous application of models C1 and C2 with arbitrary kinetic model of particles (D1–D3) is needed to express particle influence on the melt flow. The more precise model of bubble distribution, capable of predicting both the amount and composition of bubbles in the melter and at the melter exit, is on the left side of the scheme. The distribution of redox components influencing bubble behavior (box C3), is calculated prior to calculate the growth, dissolving, and rising multicomponent bubbles (box D4), as well as their distribution in the melting space using tracing technique (box C4). The distribution of particles in the melter, at the exit (melt quality), or on its bottom (quality of the vitrification process) is a result of the complex model application.

The example of application of the complex model to provide a picture of sand dissolution in the space is shown in Fig. 4 (application of boxes C1, C2, and D2). The progress in sand dissolution along the horizontal melting furnace is demonstrated by Fig. 5, where the log of particle number density in

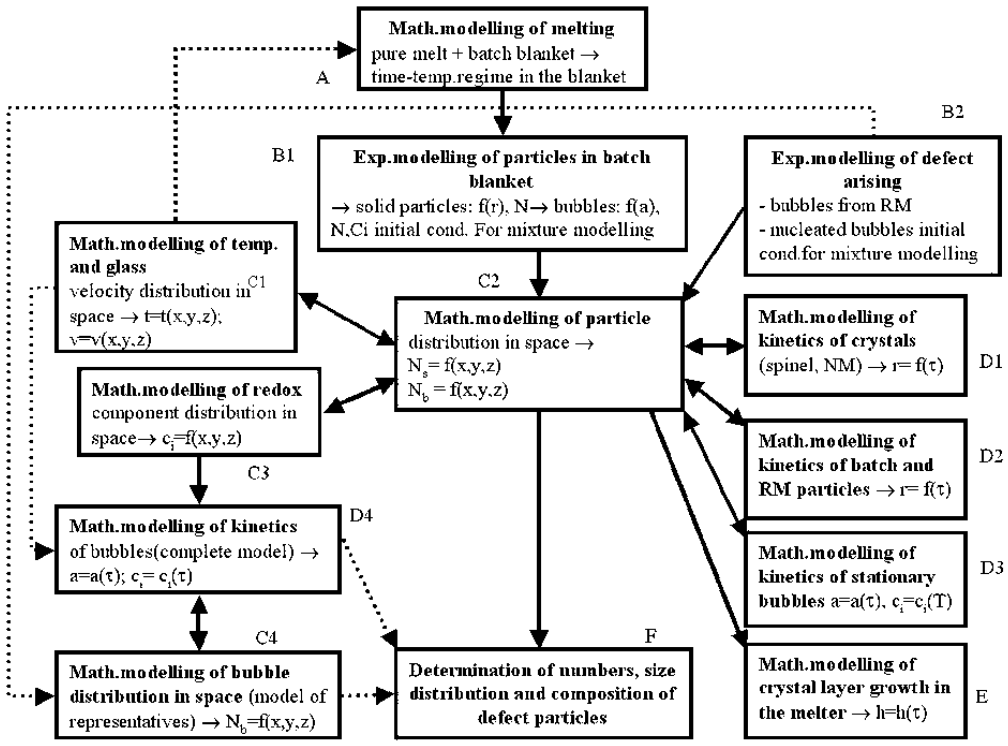

Scheme 1 Complex model of glass melting in terms of glass quality.

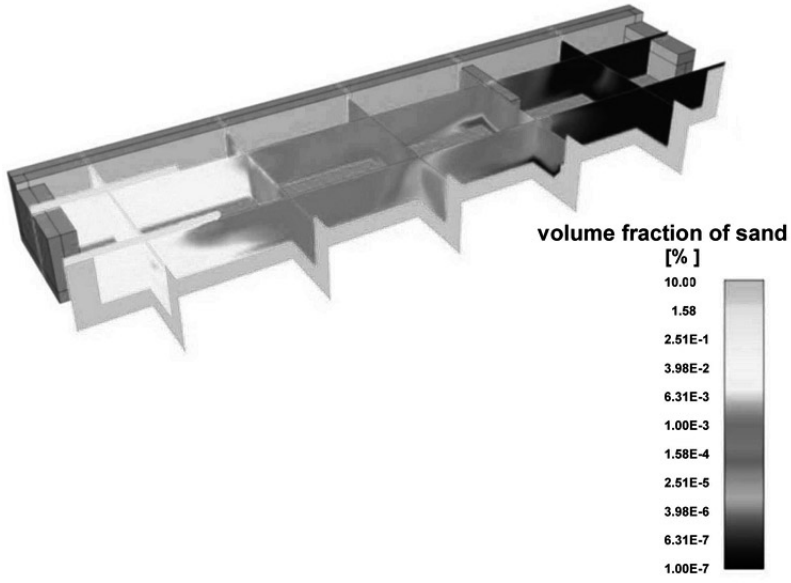

Fig. 4 Sand particle distribution in sections through the model melting space (X_0 = 16 m, Y_0 = 4 m, Z_0 = 1 m) when melting soda-lime-silica glass.

cross-section plates of 1-m thickness are plotted against the space length. The influence of sand particles on the melt flow was negligible.

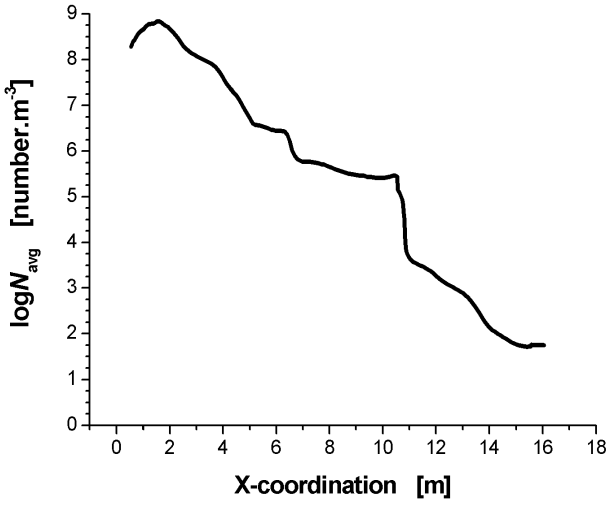

Fig. 5 Sand particle number densities in cross-section plates having thickness 1 m against the space length.

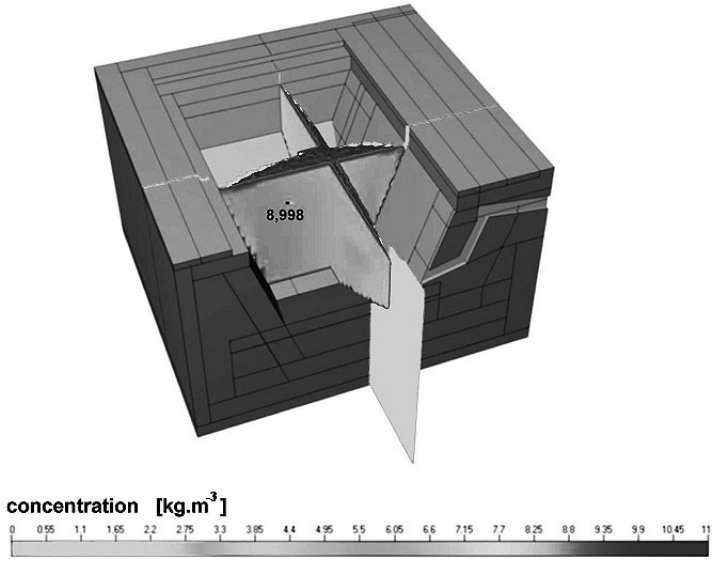

Fig. 6 Distribution of spinel crystals in sections through the HLW melter.

The almost homogeneous distribution of spinel crystals, coming from the batch, in an HLW vitrification space is obvious from Fig. 6 (boxes C1, C2, and D1). The growth of the crystal layer thickness with the initial size of crystals is show in Fig. 7.

The simplified model of bubble kinetics uses experimental values of bubble behavior (bubble growth and dissolution rates), thus avoiding the laborious measurements of gas concentrations, solubilities, and diffusivities in the melt. Its substantial disadvantage is the identical, s.c. stationary compositions of all bubbles. The distribution of stationary bubbles in the melting space obtained by using models in boxes C1, C2, and D3 is presented in Fig. 8. The impact of bubble buoyancy force on glass flow was taken into account.

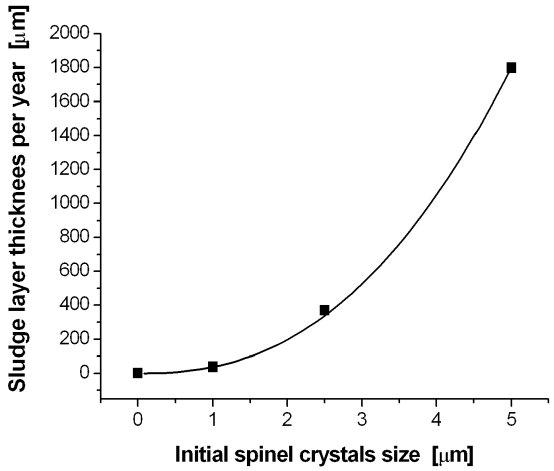

Fig. 7 Growth of the crystal layer thickness with the initial size of crystals.

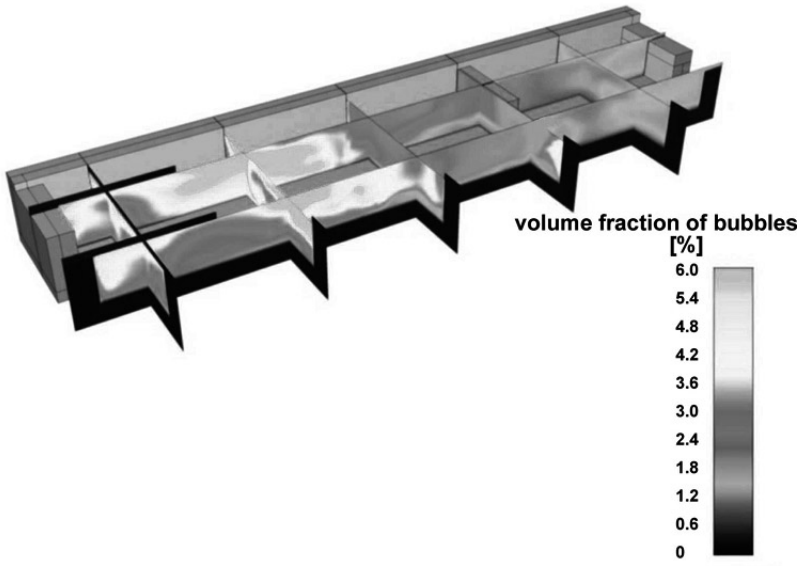

Fig. 8 Distribution of stationary bubbles in the melting space obtained by using models in boxes C1, C2, and D3.

The last bubble model cannot be used for the identification of different defect bubble sources in the space. To get the reliable spectrum of bubbles at the furnace exit, the complete bubble model has to be applied. In the case of soda-lime-silica glass, the distribution of components of two oxidation–reduction reactions should be calculated by means of the diffusive–convection equation and equations describing melt behavior (boxes C1, C2, and C3):

$$SO_4^{2-}(l) \rightleftarrows SO_2(g,l) + \tfrac{1}{2}O_2(l) + O^{2-}(l)$$

$$4Fe^{3+}(l) + 2O^{2-}(l) \rightleftarrows 4Fe^{2+}(l) + O_2(l) \qquad (11a,b)$$

As an example, the distribution of dissolved oxygen in the model melting space is presented in Fig. 9. The calculation does not involve the extraction of gases by bubbles from the melt, obvious at higher bubble densities.

The complete model of bubble behavior (box D4) involves mass transport of CO_2, N_2, H_2O, Ar, O_2, and SO_2 between bubbles and melt and together with bubble multitude tracing (box C4) provides a picture of bubble number, size, and composition distribution in the melting space and at its exit. The bubble amount and properties at the furnace exit are particularly significant as they provide information about defect bubble sources. Figure 10, for example, gives the bubble composition distribution at the furnace exit if the ratio between CO_2 and N_2 present in bubbles is taken into account. The low value of the CO_2/N_2 ratio reveals usually air sources of bubbles (mechanical bubbles, bubbles from refractory materials), the high ratio CO_2/N_2 gives evidence of melting bubbles or bubbles coming from carbon contaminations in glass.

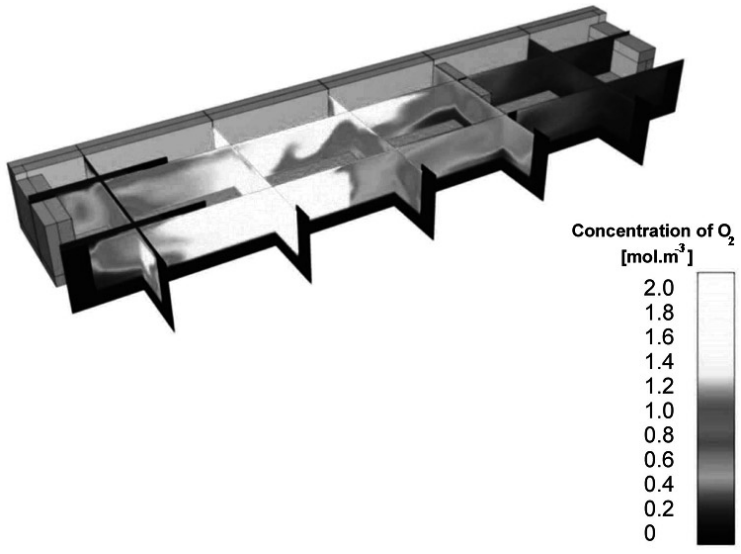

Fig. 9 Distribution of dissolved oxygen in the model melting space.

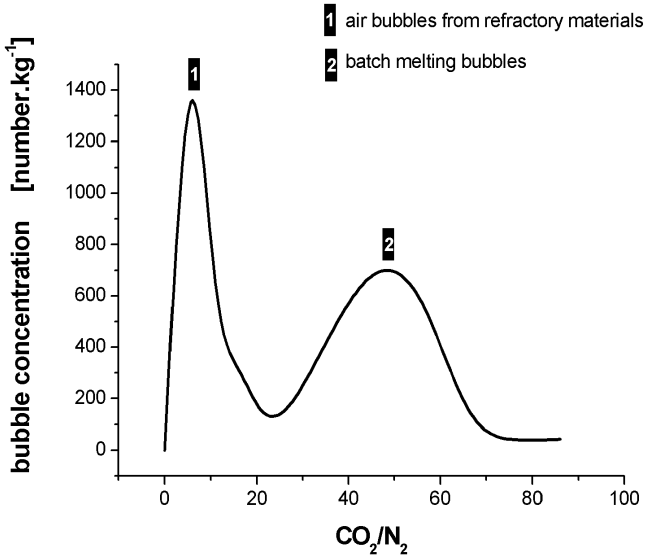

Fig. 10 Bubble composition distribution at the furnace exit if the ratio between CO_2 and N_2 present in bubbles is taken into account.

CONCLUSION

At present, the engineering and chemistry of industrial glass melting leaves its passive role of process description under real conditions. The new requirements for modern melting facilities apply for a priori determined optimum conditions of the process. This first step of the melting process development may be obtained from the process analysis, based mostly on published data. When applying the estimated optimum conditions, the simplified models of the melting and vitrification process, working at isothermal and simple glass flow conditions, appear to be the beneficial second step of active modeling. The last step of this approach tries to transfer advantageous melting regimes to real melting spaces by using complex mathematical models, particularly the models of melt containing a multitude of inhomogeneities.

ACKNOWLEDGMENT

This work was supplied with the subvention by Grant Agency of AS CR, Project No. S4032103.

REFERENCES

1. M. K. Choudhary. *Challenges and Opportunities for Glass Melting Technologies: A Transport Phenomena Perspective, Proceedings of the VI. International Seminar on Mathematical Modeling and Advanced Numerical Methods in Furnace Design and Operation*, p. 1, 28–29 June 2001, Velké Karlovice, Czech Republic (2001).
2. L. Němec. *Glastechn. Ber. Glass Sci. Technol*. **68** (1), 1 (1995).
3. L. Němec. *Anal. Model. Glass Melting, Ceramics-Silikáty* **38** (1), 45 (1994).
4. M. Hájek. *Microwave melting of glass (Czech), Skláš a Keramik* **49** (11), 281 (1999).
5. A. W. Hixon and J. H. Crowell. *Ind. Eng. Chem*. **23** (8), 923 (1931).
6 J. Matyáš, L. Němec, J. Kloužek, M. Trochta. *Spinel Settling in HLW Melters, Proceedings of the ICEM´01, 8th International Conference on Radioactive Waste Management and Environmental Remediation*, Bruges, Belgium, 30 Sept.– 4 Oct. 2001 (CD ROM).
7. To be published.
8. J. Kloužek and L. Němec. *Glasstechn. Ber. Glass Sci. Technol*. **73** (11), 329 (2000).
9. H. De Waal. *Glass Making in a Changing Society: Proceedings of the XXI International Congress on Glass*, Vol. 1, Invited Lectures, p. 145, Beijing (China) 9–14, October (1995).
10. J. L. Barton. *Present Trends in Industrial Glass Making: Proceedings of the XXI International Congress on Glass*, Vol. 1, Invited Lectures, Beijing (China), p. 233, 9–14 October (1995).